APE1/Ref-1 facilitates recovery of gray and white matter and neurological function after mild stroke injury

R. Anne Stetler[a,b,c], Yanqin Gao[a,b], Rehana K. Leak[d], Zhongfang Weng[b,c], Yejie Shi[b,c], Lili Zhang[b,c], Hongjian Pu[b], Feng Zhang[a,b,c], Xiaoming Hu[a,b,c], Sulaiman Hassan[b,c], Carolyn Ferguson[e,f], Gregg E. Homanics[e,f], Guodong Cao[a,b,c], Michael V. L. Bennett[a,g,1], and Jun Chen[a,b,c,1]

[a]State Key Laboratory of Medical Neurobiology and Institutes of Brain Science, Fudan University, Shanghai 200032, China; [b]Pittsburgh Institute of Brain Disorders & Recovery, Department of Neurology, University of Pittsburgh, Pittsburgh, PA 15213; [c]Geriatric Research, Education and Clinical Center, Veterans Affairs Pittsburgh Health Care System, Pittsburgh, PA 15261; [d]Division of Pharmaceutical Sciences, Mylan School of Pharmacy, Duquesne University, Pittsburgh, PA 15282; [e]Department of Anesthesiology, University of Pittsburgh, Pittsburgh, PA 15261; [f]Department of Pharmacology and Chemical Biology, University of Pittsburgh, Pittsburgh, PA 15261; and [g]Dominick P. Purpura Department of Neuroscience, Albert Einstein College of Medicine, Bronx, NY 10461

Contributed by Michael V. L. Bennett, April 29, 2016 (sent for review March 6, 2016; reviewed by Cesario Borlongan and Chia-Yi Kuan)

A major hallmark of oxidative DNA damage after stroke is the induction of apurinic/apyrimidinic (AP) sites and strand breaks. To mitigate cell loss after oxidative DNA damage, ischemic cells rapidly engage the base excision-repair proteins, such as the AP site-repairing enzyme AP endonuclease-1 (APE1), also named redox effector factor-1 (Ref-1). Although forced overexpression of APE1 is known to protect against oxidative stress-induced neurodegeneration, there is no concrete evidence demonstrating a role for endogenous APE1 in the long-term recovery of gray and white matter following ischemic injury. To address this gap, we generated, to our knowledge, the first APE1 conditional knockout (cKO) mouse line under control of tamoxifen-dependent Cre recombinase. Using a well-established model of transient focal cerebral ischemia (tFCI), we show that induced deletion of APE1 dramatically enlarged infarct volume and impaired the recovery of sensorimotor and cognitive deficits. APE1 cKO markedly increased postischemic neuronal and oligodendrocyte degeneration, demonstrating that endogenous APE1 preserves both gray and white matter after tFCI. Because white matter repair is instrumental in behavioral recovery after stroke, we also examined the impact of APE1 cKO on demyelination and axonal conduction and discovered that APE1 cKO aggravated myelin loss and impaired neuronal communication following tFCI. Furthermore, APE1 cKO increased AP sites and activated the prodeath signaling proteins, PUMA and PARP1, after tFCI in topographically distinct manners. Our findings provide evidence that endogenous APE1 protects against ischemic infarction in both gray and white matter and facilitates the functional recovery of the central nervous system after mild stroke injury.

ischemia | neurodegeneration | base excision repair | oxidative DNA damage | white matter injury

Focal ischemic injury in the brain is both a spatial and temporal event, wherein the infarct zone expands gradually over several days (1, 2). However, if the stroke insult is moderate, the periinfarct regions may recover over time. The spontaneous recovery of periinfarct structures and neurological functions creates an opportunity to research the molecular mechanisms underlying endogenous neuroprotection and neural repair, which may accelerate the discovery of rational therapeutic targets for stroke treatment.

Oxidative DNA damage (ODD) is an early event following cerebral ischemia and reperfusion (3, 4), and reversal of ODD in penumbral regions is associated with eventual recovery from such insult (4, 5). Repair of ODD by the base excision-repair (BER) pathway targets oxidized DNA base lesions through a multistep process. First, base lesions are recognized by DNA glycosylases, which cleave the damaged bases and form temporary apurinic/apyrimidinic (AP) sites. The AP sites are then recognized by the critical BER enzyme, AP endonuclease-1/redox effector factor-1 (referred to here as APE1) (6, 7). APE1 repairs AP sites by cleaving the phosphodiester backbone 5′ to the AP site and thus creating a 3′-OH group and a 5′-deoxyribose phosphate residue that is the preferred substrate for DNA polymerase-β (6–8). As one of the major steps in BER, APE1 subsequently facilitates the engagement of DNA polymerase-β and DNA ligase I or III (8). Inadequate repair capacity leads to the accumulation of unrepaired AP sites (9) and is associated with inexorable progression of the ischemic injury (3). We and others have demonstrated that enhanced APE1 activity by means of transgenic overexpression or APE1 expression-inducing peptides, such as the pituitary adenylate cyclase-activating polypeptide (PACAP), confers robust neuroprotection against ischemic brain injury (10–12). Furthermore, a strong correlation exists between loss of APE1 expression in ischemic neurons and neuronal cell death after ischemia (9, 13–15). Energy failure after ischemia has been speculated to deplete APE1 expression, thereby triggering neuronal death (16). However, the role of endogenous APE1 in cellular protection from ischemic injury has not been unequivocally established, as knockout of this enzyme leads to catastrophic deficiencies in neurogenesis and is lethal embryonically (15, 17).

Significance

AP endonuclease-1 (APE1)/redox effector factor-1 (Ref-1) is an essential DNA repair enzyme that has been difficult to study mechanistically because of embryonic lethality in conventional knockout animals. Thus, we generated a conditional APE1 knockout model to examine the protective role of endogenous APE1 in experimental stroke. Induced APE1 knockout in adulthood greatly exacerbated neuron and oligodendrocyte loss after mild ischemic stroke and prevented the intrinsic, long-term recovery of sensorimotor function and spatial learning and memory. APE1 knockout also aggravated ischemia-induced destruction of myelin and impairment of axon conduction in white matter. We conclude that APE1 dictates fundamental life and death decisions in both gray and white matter and plays an indispensable role in intrinsic recovery after mild ischemic injury.

Author contributions: R.A.S., Y.G., G.E.H., G.C., M.V.L.B., and J.C. designed research; R.A.S., Z.W., Y.S., L.Z., H.P., F.Z., S.H., C.F., and G.C. performed research; R.A.S., Y.G., R.K.L., Y.S., X.H., M.V.L.B., and J.C. analyzed data; and R.A.S., R.K.L., Y.S., M.V.L.B., and J.C. wrote the paper.

Reviewers: C.B., University of South Florida; and C.-Y.K., Emory University School of Medicine.

The authors declare no conflict of interest.

Freely available online through the PNAS open access option.

[1]To whom correspondence may be addressed. Email: michael.bennett@einstein.yu.edu or chenj2@upmc.edu.

This article contains supporting information online at www.pnas.org/lookup/suppl/doi:10.1073/pnas.1606226113/-/DCSupplemental.

www.pnas.org/cgi/doi/10.1073/pnas.1606226113

Concrete evidence has been lacking thus far to establish a role for endogenous APE1 in long-term functional recovery following mild neural injury. Furthermore, the mechanisms that underlie cell death as a result of the accumulation of unrepaired ODD are still poorly understood. To assess the role of endogenous APE1 in protection from ischemic injury, we generated, to our knowledge, the first APE1 conditional knockout (cKO) mouse line under the control of a tamoxifen-inducible Cre recombinase. Our findings reveal that the accumulation of ODD and the activation of pro-death programs in tamoxifen-treated APE1 cKO mice are markedly increased in neurons and oligodendrocytes after a transient cerebral ischemic insult, augmenting injury in both gray and white matter and exacerbating behavioral outcomes. These data highlight an important role for endogenous APE1 in innate protective mechanisms in gray and white matter following cerebral ischemia and reperfusion, and suggest that DNA repair through the BER pathway is an essential step for the spontaneous recovery of behavioral function following ischemic injury.

Results

Induced Knockout of APE1 Potentiates Cerebral Ischemic Injury. Previous attempts at global knockout of the APE1 gene resulted in embryonic lethality on embryonic days (E)5 to E9 (15, 17). Thus, a conditional APE1 knockout mouse line was created by insertion of *loxP* sites around exons IV and V of the *Apex1* gene (details are provided in *SI Methods*) (Fig. S1). The homozygous APE1$^{flox/flox}$ mice were viable, fertile, and normal in size and did not exhibit any gross physical or behavioral abnormalities. APE1$^{flox/flox}$ mice were then crossed with hemizygous CAGGCre-ER mice carrying tamoxifen-inducible, ubiquitously expressed Cre-recombinase (18) to generate mice of which 50% were CAGGCre-ER; APE1$^{flox/wt}$ (Fig. S2*A*). These mice were bred to APE1$^{flox/flox}$ mice, yielding offspring of which 25% had the genotype CAGGCre-ER; APE1$^{flox/flox}$ (Fig. S2*C*). Mice with the genotype CAGGCre-ER; APE1$^{wt/wt}$ served as controls (Fig. S2*B*) and received the same tamoxifen treatment. In the following text and figures, APE1 cKO and APE1 WT are used to refer to the CAGGCre-ER; APE1$^{flox/flox}$ and CAGGCre-ER; APE1$^{wt/wt}$ mice, respectively, both after tamoxifen treatment. To induce Cre-mediated recombination, tamoxifen was administered (75 mg/kg, i.p.) for 5 d at 8–12 wk of age, which effectively decreased APE1 protein expression in various brain regions of APE1 cKO mice (Fig. S2*D*). Furthermore, lysates derived from APE1 cKO brains were ineffective in repairing AP sites in an in vitro DNA repair assay (Fig. S2*E*). Thus, the APE1 cKO mice showed not only ablated APE1 gene expression in the brain, but also suppressed intrinsic DNA repair activity through the BER pathway.

We evaluated the effect of conditional APE1 knockout on stroke outcomes to indirectly test the hypothesis that the accumulation of AP sites in the ischemic brain worsens neurological outcomes after cerebral ischemia. Transient focal cerebral ischemia (tFCI) was induced in mice for either 30 or 60 min by means of middle cerebral artery occlusion. Physiological parameters, including core temperature and blood gases, were maintained in the normal range in all groups during tFCI. Regional cerebral blood flow (CBF) was measured by 2D laser-speckle imaging during tFCI until 45 min following reperfusion onset. The ischemic core and penumbral regions during tFCI (defined as regional CBF < 20% and between 20% and 35% of preischemic baseline, respectively) were of equivalent sizes in APE1 cKO and APE1 WT brains (Fig. 1*A*), confirming that the initial insult was of the same magnitude in both genotypes. The ischemic infarct in APE1 WT mice was limited to the striatum 48 h after 30 min of tFCI, whereas the infarct encompassed both the striatum and the frontal-parietal cortex 48 h after 60 min of tFCI (Fig. 1 *B* and *C*). As expected, infarct volume was dramatically increased in APE1 cKO mice compared with APE1 WT mice after either 30 or 60 min of tFCI (Fig. 1 *B* and *C*). We also observed a significant increase in mortality in the APE1 cKO mice (recorded up to 28 d after 60 min of tFCI) (Fig. 1*D*). These findings suggest that endogenous APE1

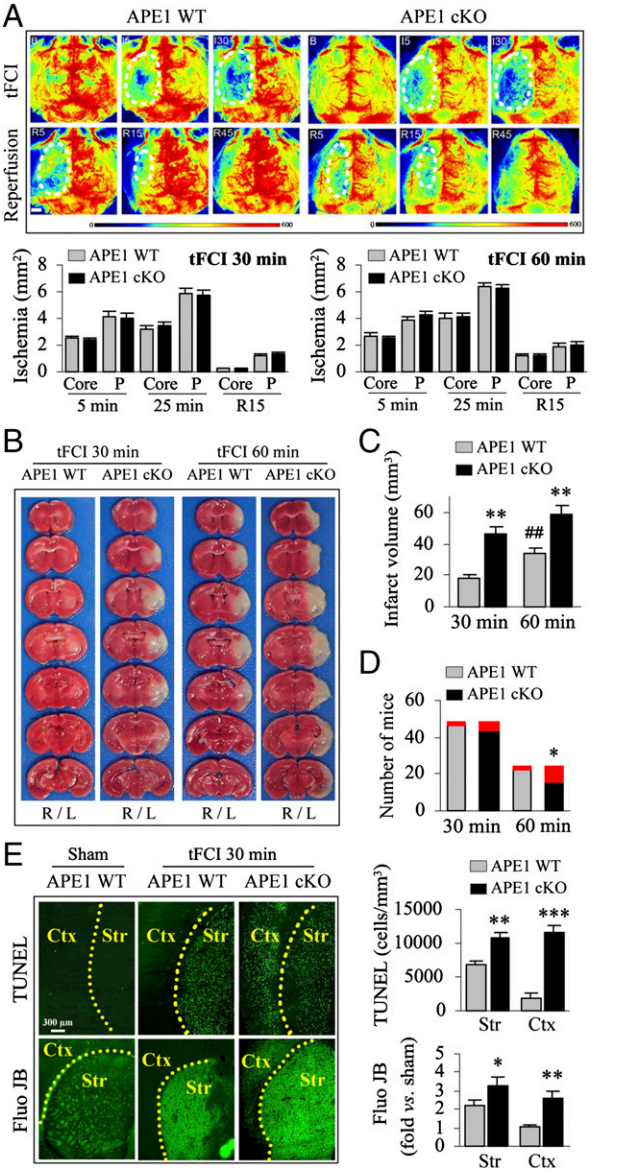

Fig. 1. Induced knockout of APE1 increases infarct volumes, mortality, and cell death after tFCI. tFCI was induced in tamoxifen-treated CAGGCre-ER; APE1$^{wt/wt}$ (APE1 WT) and CAGGCre-ER; APE1$^{flox/flox}$ (APE1 cKO) mice. (*A*) Cerebral blood flow was assessed by 2D laser-speckle imaging. Representative images show the control, the ischemic area (depicted by the dotted line) during 5 and 30 min of tFCI and after 5, 15, and 45 min of reperfusion following 60 min of tFCI. (Scale bar, 1 mm.) The bar graphs show ischemic areas at 5 and 25 min in both the ischemic core (defined as CBF < 20% of preischemia baseline) and penumbra (P) (CBF = 20–35% of preischemia baseline) during 30 or 60 min of tFCI or 15 min of reperfusion. The results reveal similar CBF changes in APE1 WT and APE1 cKO mice. $n = 5$ per group. (*B* and *C*) Infarct volume was assessed at 48 h after tFCI by TTC (2,3,5-triphenyltetrazolium) staining (the right and left hemispheres are labeled with R and L, respectively) and quantified as described using ImageJ under blinded conditions. Values are means ± SEM, $n = 8$ per group. $^{**}P \leq 0.01$ vs. the matched APE1 WT group. $^{\#\#}P \leq 0.01$ vs. 30 min WT group. (*D*) The number of animals that survived (bottom portion of bars) or died (upper red portion of bars) by 28 d after tFCI. Comparisons of animal survival rates were performed by Kaplan–Meier survival analysis. $^{*}P \leq 0.05$ vs. the matched APE1 WT group. (*E*) Histological assessments of cell death were performed at 48 h after tFCI (30 min) using the TUNEL stain for DNA fragmentation and Fluoro-Jade B (Fluo JB) for cell degeneration, respectively. TUNEL^{+} cells were counted using stereology, and Fluoro-Jade B was semiquantified by measuring the fluorescence intensity in the striatum (Str) and cortex (Ctx). Values are mean ± SEM, $n = 6$ per group. $^{**}P \leq 0.01$, $^{***}P \leq 0.001$ vs. the matched APE1 WT group.

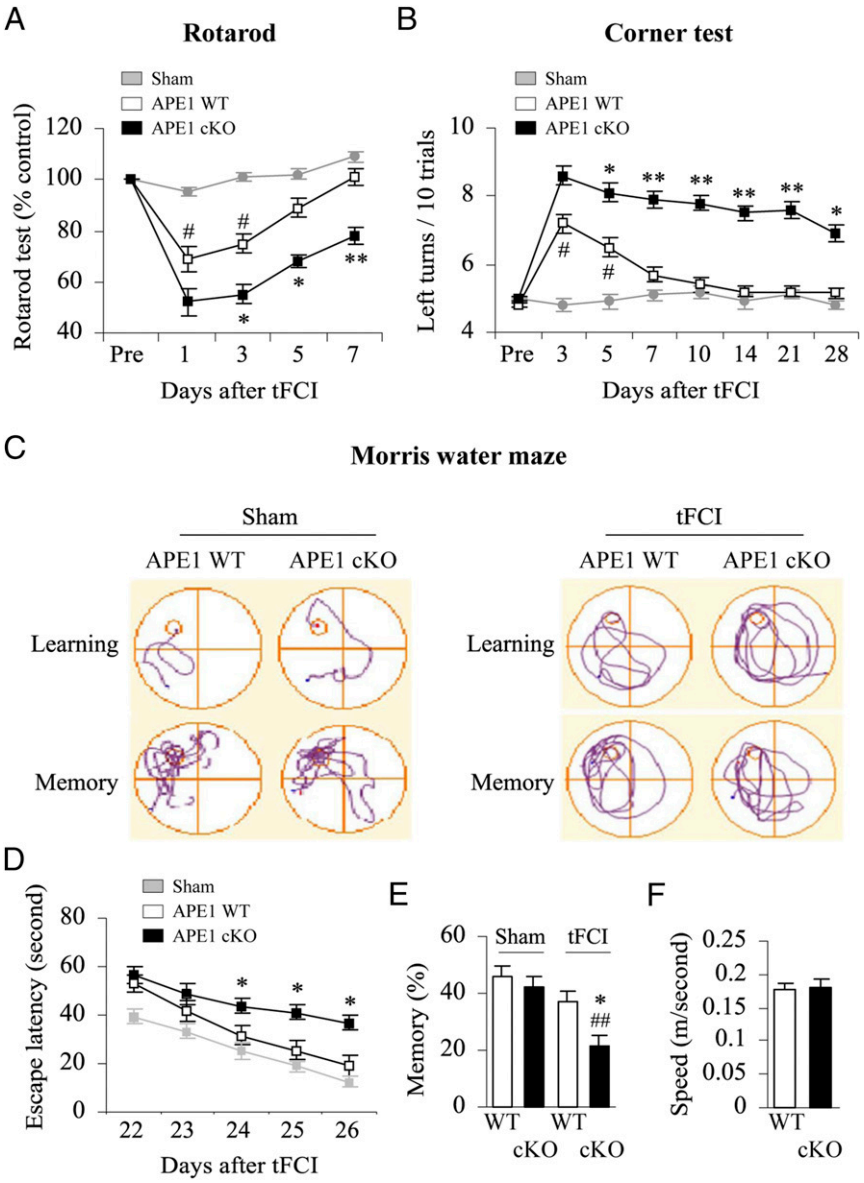

Fig. 2. APE1 deficiency impairs sensorimotor and cognitive recovery after tFCI. In sham control animals, neither the sensorimotor function tests (rotarod test, corner test) nor the cognitive test (Morris water maze) revealed significant difference between the APE1 WT and APE1 cKO mice. Thus, the "sham group" in *A*, *B*, and *D* refers to the combination of both APE1 WT and APE1 cKO genotypes. (*A*) Rotarod performance was measured every other day for the first week following 30 min of tFCI. The latency to fall after ischemic injury was normalized to latency before the induction of ischemia. $n = 6$–8 per group. $^{*}P \leq 0.05$; $^{**}P \leq 0.01$ vs. the matched APE1 WT group; $^{\#}P \leq 0.05$ vs. the sham group. (*B*) The corner test was performed up to 28 d following 30 min of tFCI. The number of left turns per 10 trials was recorded and plotted. The sham control group showed no turning bias or asymmetry (average of 5 left turns/10 trials); the postischemic mice showed increased turning toward the body side with unaffected mobility (left, ipsilateral to the ischemic hemisphere). The APE1 WT mice showed complete recovery by 7–10 d, whereas the APE1 cKO mice showed only partial recovery by 28 d. $n = 6$–8 per group. $^{*}P \leq 0.05$; $^{**}P \leq 0.01$ vs. the matched APE1 WT group; $^{\#}P \leq 0.05$ vs. the sham group. (*C*–*F*) Long-term cognitive functions were assessed by the Morris water maze at 22–27 d after 30 min of tFCI. $n = 8$–10 per group. Shown are the mean ± SEM $^{*}P \leq 0.05$ vs. the matched APE1 WT group; $^{\#\#}P \leq 0.01$ vs. the sham group. (*C*) Representative swim path traces (24–26 d after tFCI) of mice attempting to find a hidden platform (top traces, "learning"), or searching for the platform after its removal (bottom traces, "memory"). (*D*) The escape latency (i.e., time needed to discover the platform) was recorded on days 22–26 after tFCI. (*E*) Memory was tested at 27 d after tFCI. The percentage of time spent in the target quadrant after the platform was removed was plotted to reflect memory. (*F*) Swimming speed was assessed at 27 d after tFCI for each genotype, to ensure that the observed differences did not reflect compromised swimming abilities.

reduces the consequences of DNA damage. To avoid potential confounds from exclusion of animals in the APE1 cKO group because of high mortality, we used the 30-min tFCI model for further experiments. Use of the milder injury also allowed us to examine whether APE1 contributes to recovery of neurological function in otherwise untreated animals.

Consistent with the hypothesis that APE1 rescues cells from ischemic injury, APE1 cKO mice exhibited greater numbers of degenerating TUNEL^{+} and Fluoro-Jade^{+} profiles at 48 h after 30 min of tFCI. In APE1 WT mice, ischemia-induced cell death was prominent in the striatum but modest in the cortex; in APE1 cKO mice, ischemic cell death was significantly potentiated in both striatum and cortex, consistent with expansion of the infarct region (Fig. 1*E*). These results support the conclusion that APE1 attenuates the consequences of ischemic brain injury.

To determine if loss of endogenous APE1 worsens neurofunctional outcomes after cerebral ischemia, we subjected APE1 cKO and APE1 WT mice to 30 min of tFCI and performed behavioral

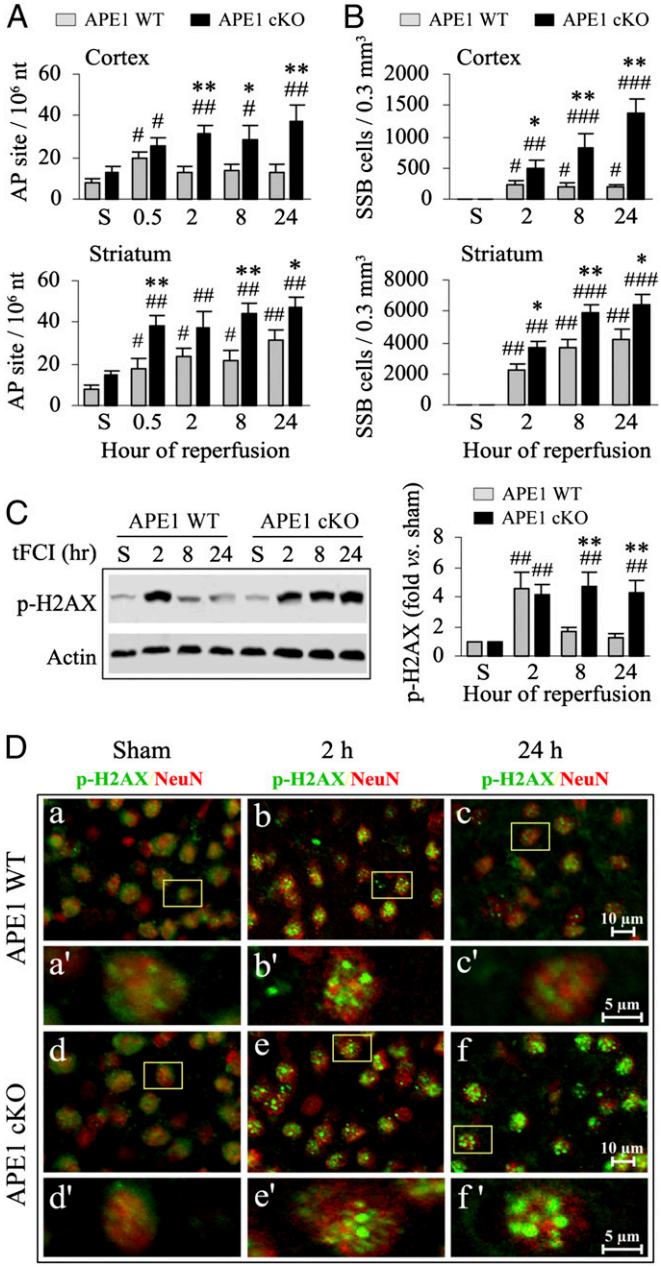

Fig. 3. APE1 deficiency increases the accumulation of ODD after tFCI. (*A*) AP site frequency was quantitatively measured in cortical and striatal extracts, respectively, from APE1 WT and APE1 cKO mice under sham condition (S) or at 0.5, 2, 8, and 24 h after 30 min of tFCI. Data are expressed as the number of AP site per 10^6 nucleotides. (*B*) SSBs were detected immunohistochemically using the PANT assay, and positively labeled cells were counted using stereology at the indicated time points after 30 min of tFCI. Values are means ± SEM, $n = 6$ per group. $^{*}P \leq 0.05$; $^{**}P \leq 0.01$ vs. the matched APE1 WT group; $^{\#}P \leq 0.05$; $^{\#\#}P \leq 0.01$; $^{\#\#\#}P \leq 0.001$ vs. the sham group. (*C*) Levels of phospho-H2AX (marker of genomic damage) were assessed in cortical lysates by Western blotting at 2, 8, and 24 h after tFCI. $n = 4$ per group. $^{**}P \leq 0.01$ vs. the matched APE1 WT group; $^{\#\#}P \leq 0.01$ vs. the sham group. (*D*) Double-label immunofluorescent staining for p-H2AX (green) and the neuronal marker NeuN (red) in the cortices of sham controls and at 2 or 24 h after tFCI (*a–c*, APE1 WT; *d–f*, APE1 cKO mice). High-magnification images from the boxed regions revealed distinctly punctate patterns of p-H2AX immunofluorescence in postischemic cortical neurons (*a′–c′*, APE1 WT; *d′–f′*, APE1 cKO mice). The frequency of punctate p-H2AX immunofluorescence subsided to control levels at 24 h after tFCI in APE1 WT brain, but remained elevated at 24 h after tFCI in APE1 cKO brains.

assessments at various times after reperfusion: including the rotarod test (1–7 d), corner test (3–28 d), and Morris water maze (22–27 d). According to the rotarod and corner test results, postischemic APE1 WT mice were indistinguishable from sham control animals by 7 d after tFCI, consistent with previous observations that mild ischemia-challenged mice rapidly recover sensorimotor function. Induced deletion of APE1 significantly worsened postischemic neurobehavioral performance compared both to sham controls and postischemic APE1 WT mice throughout the testing period (Fig. 2 *A* and *B*). In addition, spatial learning and memory in the Morris water maze—which depend partially on hippocampal integrity—were significantly worse in postischemic APE1 cKO mice compared with postischemic APE1 WT mice. That is, APE1 cKO increased the amount of time within a trial that the mouse needed to find the hidden platform (impaired learning), as well as decreased the percentage of time spent swimming in the target quadrant when the platform had been removed after the learning period (impaired memory) (Fig. 2 *C–E*). This degree of spatial memory impairment is not typically observed in the 30-min tFCI model, as shown by the lack of difference between postischemic APE1 WT mice and sham controls (Fig. 2 *C–E*). No differences between postischemic groups were observed in swim speed at 27 d after tFCI (Fig. 2*F*), indicating that gross motor differences did not confound the interpretation of APE1 knockout effects on spatial learning and memory. The cognitive deficits observed over the extended survival period correlated with histological damage in striatum and cortex, as there was greater loss of microtubule-associated protein 2 (MAP2) staining in the APE1 cKO mice compared with APE1 WT mice at 28 d following 30 min of tFCI (Fig. S3). Taken together, these data demonstrate that loss of endogenous APE1 protein increases cellular damage and potentiates sensorimotor and cognitive impairments following cerebral ischemic insults, in support of a significant role for APE1 in the mitigation of ischemic injury.

APE1 Deficiency Potentiates the Accumulation of ODD Following Mild Ischemic Injury. Acute ODD has long been associated with cell injury, and the accumulation of unrepaired ODD in response to cytotoxic stimuli, including ischemia, engages cell death cascades (1, 3, 19). As APE1 is an essential component of the DNA BER process, loss of APE1 activity is expected to lead to robust accumulation of ODD in cells after ischemia with reperfusion. Using three distinct measures of ODD, we verified that induced knockout of APE1 led to significant increases in ODD in the postischemic brain. Tissues collected from postischemic cortex and striatum, respectively, were quantitatively assessed for the number of AP sites and cells containing DNA single strand breaks (SSB) using the ELISA and DNA polymerase I-mediated biotin-dATP nick-translation (PANT) assay (3), respectively. In postischemic APE1 WT mice, AP sites (Fig. 3*A*) and SSB-containing cells (Fig. 3*B*) were increased early (0.5 h of reperfusion) after 30 min of tFCI in both the striatum and cortex. For at least 24 h thereafter, AP sites and SSB-containing cells remained elevated over sham controls in the striatum but subsided near to sham control levels in the cortex, reflecting an effective intrinsic recovery process in the postischemic cortex of APE1 WT mice. In contrast, AP sites and SSB-containing cells were remarkably elevated in both the postischemic striatum and cortex in APE1 cKO mice throughout the 24-h reperfusion timeframe, and ODD levels were significantly increased compared with the APE1 WT mice in both brain regions (Fig. 3 *A* and *B*). Because the increase in AP sites in the cortex is sustained instead of transient following loss of APE1, we conclude that APE1 facilitates recovery from DNA damage in gray matter.

H2AX, a member of the histone H2A family, is a DNA damage-sensing protein that is activated by phosphorylation at Serine 139, and this phosphorylated H2AX (p-H2AX) can be detected immunohistochemically as dense foci in nucleosomes (20). The levels of p-H2AX were significantly increased in the postischemic cortex 2 h after 30 min of tFCI in the APE1 WT mice, but subsided

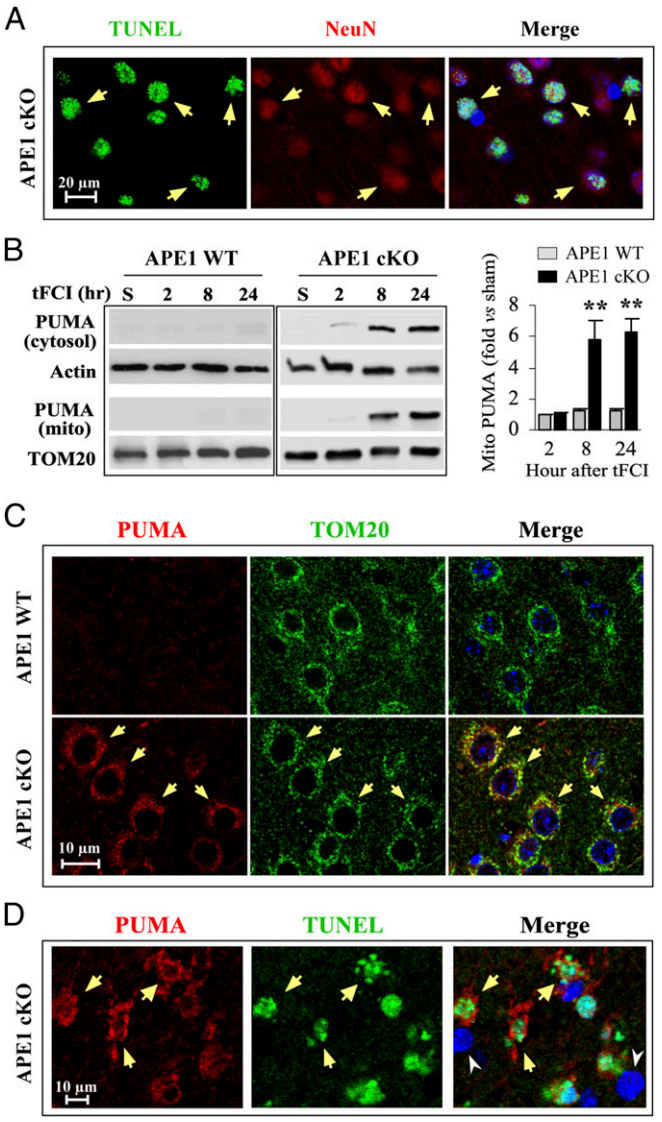

Fig. 4. APE1 deficiency activates proapoptotic PUMA signaling in postischemic neurons. (*A*) Representative images demonstrating TUNEL (green, arrows) colabeling with the neuronal marker NeuN (red, arrows) in the postischemic cortex of an APE1 cKO mouse 24 h following 30 min tFCI. DAPI (blue, in merged image) staining was used to identify cell nuclei. (*B*) Levels of PUMA in total protein extracts and the mitochondrial fraction of cortical tissue were assessed by Western blotting after sham operation or at 2, 8, and 24 h after tFCI. β-Actin and TOM20 (a mitochondria-specific protein) served as the loading controls for whole cell protein extracts and the mitochondrial fraction, respectively. Data are presented as mean± SEM, fold-changes versus sham controls. $n = 4$ per group. $^{**}P \leq 0.01$ vs. the matched APE1 WT group. (*C*) Triple-label immunofluorescent staining for PUMA (red), TOM20 (green), and DAPI (blue, in merged images only) in the postischemic cortex at 8 h following 30 min of tFCI in APE1 WT (*Upper*) and APE1 cKO (*Lower*) mice. PUMA immunofluorescence was increased and was closely associated with TOM20 (arrows) in postischemic cortical neurons of APE1 cKO brains, but not of APE1 WT brains. (*D*) Close association of intense PUMA immunofluorescence (red, arrows) with TUNEL$^+$ staining (green, arrows) in the ischemic cortex 24 h after 30 min of tFCI in an APE1 cKO brain. Cell nuclei were stained with DAPI in the merged image. Two TUNEL$^-$ cells were also immunonegative for PUMA (arrowheads).

to control levels within 8 h (Fig. 3*C*), again consistent with an intrinsic recovery process for ODD in the postischemic cortex. APE1 cKO mice exhibited similar p-H2AX levels in the postischemic cortex as APE1 WT mice at 2 h following 30 min of tFCI, but had significantly higher p-H2AX levels at 8 and 24 h following reperfusion, suggesting impaired recovery from ODD (Fig. 3*C*). Double-label immunofluorescence revealed elevated immunofluorescence of p-H2AX, exhibiting increased intensity of punctate granules in NeuN$^+$ cortical neurons of APE1 WT mice at 2 h after 30 min of tFCI, but this pattern of punctate staining was diminished by 24 h following reperfusion (Fig. 3*D*). In contrast, in APE1 cKO mice there was a similarly high level of p-H2AX immunofluorescence at 2-h reperfusion, but it persisted for at least 24 h (Fig. 3*D*). Not surprisingly, the persistent presence of DNA damage in the cortex of APE1 cKO mice closely correlates with the regional patterns of ODD induction in the forms of AP sites and SSB (Fig. 3 *A* and *B*). These findings strongly suggest that loss of APE1 interferes with the cellular recovery process in the postischemic penumbra, likely contributing to the expansion of the infarct zone to the overlying cortex (Fig. 1 *B* and *C*). Thus, induced deletion of APE1 leads to the failure of DNA repair, and the resulting accumulation of ODD correlates with potentiation of cerebral ischemic injury.

APE1 Deficiency Enhances Mitochondrial Translocation of PUMA in Apoptotic Ischemic Neurons. In our investigation of the effects of APE1 knockout on ischemic injury, we explored the extent of destruction of specific cell populations (i.e., neurons and oligodendrocytes) within ischemic brain regions following 30 min of tFCI. We found extensive colabeling of the neuronal marker NeuN with TUNEL in the cortex of APE1 cKO mice 24 h after tFCI (Fig. 4*A*). As the p53 up-regulated modulator of apoptosis (PUMA) is a proapoptotic protein whose expression is regulated by the tumor suppressor p53 as part of the DNA damage response after cerebral ischemia (21), we explored whether the exacerbation of cell death by APE1 knockout was associated with increased expression of PUMA. In sham control mice or APE1 WT mice subjected to 30 min of tFCI, PUMA was nearly undetectable by Western blot analyses in either the cytosolic or mitochondrial fraction of cerebral cortical extracts (Fig. 4*B*). However, in APE1 cKO mice subjected to 30 min of tFCI followed by 8 or 24 h of reperfusion, PUMA expression was significantly elevated in both cytosolic and mitochondrial fractions (Fig. 4*B*), which supports the notion that the accumulation of ODD because of loss of APE1 causes PUMA up-regulation in postischemic brain. The presence of PUMA in the mitochondrial fraction suggested that this protein (PUMA) is translocated into mitochondria in postischemic neurons. Indeed, double-label immunofluorescent staining exhibited a punctate pattern for PUMA that was closely associated with the mitochondrial marker TOM20 (translocase of outer membrane 20 kDa) in cortical neurons 8 h after tFCI (Fig. 4*C*). Moreover, the increased PUMA immunofluorescence was particularly evident in TUNEL$^+$ cortical cells displaying condensed and fragmented nuclei 24 h after tFCI (Fig. 4*D*). These findings support the hypothesis that the induction of PUMA may mediate the degeneration of APE1-deficient cortical neurons after ischemia and reperfusion.

Loss of APE1 Exacerbates Oligodendrocyte Cell Death and Is Associated with Poly(ADP ribose) Polymerase 1 Activation in Postischemic Brain. White matter injury (WMI) contributes significantly to both sensorimotor and cognitive neurological deficits after cerebral ischemia (22). However, the role of DNA damage and repair in ischemic WMI has been largely overlooked. The APE1 cKO brain exhibited a marked postischemic increase in the number of TUNEL$^+$ cells within white matter tracts of the corpus callosum (CC) and external capsule (EC) 48 h after 30 min of tFCI compared with the APE1 WT brain (Fig. 5 *A* and *B*). To determine the cell types undergoing apoptosis, we performed double-label immunofluorescent staining for TUNEL and cell makers for microglia/macrophages (Iba1), astrocytes (glial fibrillary acidic protein, GFAP), or mature oligodendrocytes (adenomatous polyposis coli, APC). In the CC/EC of APE1 cKO mice, the majority of TUNEL$^+$ cells expressed APC (Fig. 5 *C* and *D*). In contrast, in the CC/EC of APE1 WT postischemic mice, few APC$^+$ cells were

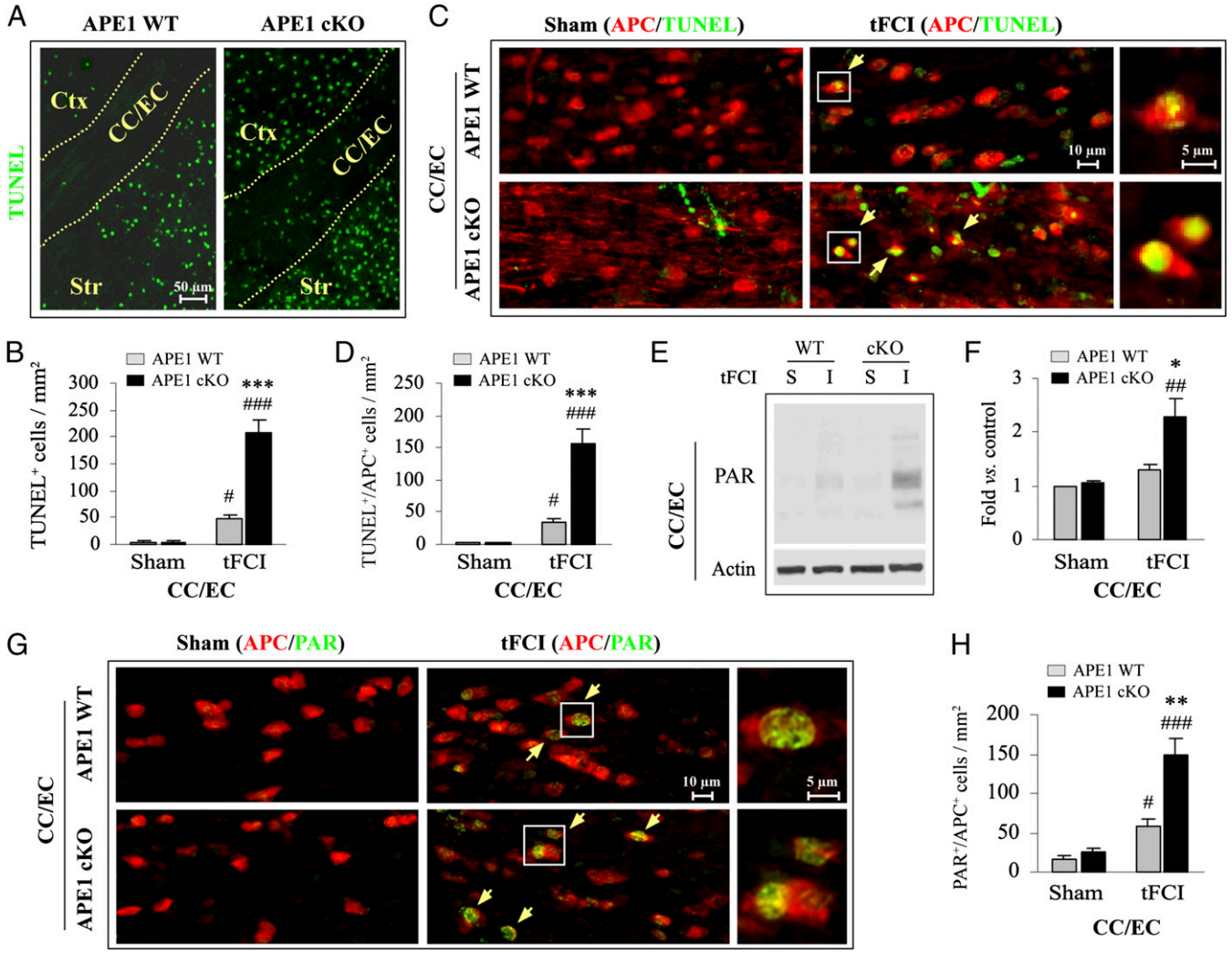

Fig. 5. APE1 deficiency activates proapoptotic PARP1 in postischemic oligodendrocytes. (*A*) TUNEL staining of brain sections at 48 h following 30 min of tFCI. Ctx, cortex; Str, striatum; CC/EC, corpus callosum and external capsule. Few TUNEL$^+$ cells could be detected in these brain regions of the APE1 cKO or APE1 WT mice after sham surgery. (*B*) The number of TUNEL$^+$ cells in the CC/EC region was quantified. $n = 6$ per group. $^{***}P \leq 0.001$ vs. the matched APE1 WT group; $^{\#}P \leq 0.05$; $^{\#\#\#}P \leq 0.001$ vs. the sham group. (*C*) Colocalization (yellow arrows) of TUNEL (green) with the mature oligodendrocytic marker APC (red) in the CC/EC in sham and 48 h following 30 min of tFCI in APE1 WT and APE1 cKO mice. (*D*) TUNEL$^+$/APC$^+$ cells were quantified from randomly selected microscopic fields in the CC/EC. $n = 6$ per group. $^{***}P \leq 0.001$ vs. the matched APE1 WT group; $^{\#}P \leq 0.05$; $^{\#\#\#}P \leq 0.001$ vs. the sham group. (*E* and *F*) Western blot analysis of PAR (marker of PARP1 activity, multiple bands) in extracts derived from CC/EC after sham operation (S) or 48 h after ischemia (I). PAR immunoblot results were as fold-changes over sham controls. $n = 4$ per group. $^{*}P \leq 0.05$ vs. the matched APE1 WT group; $^{\#\#}P \leq 0.01$ vs. the sham group. (*G* and *H*) Colocalization (yellow, arrows) of PAR (green) with APC (red) in the CC/EC at 48 h following 30 min of tFCI. PAR$^+$/APC$^+$ cells were quantified from randomly selected microscopic fields in the CC/EC. $n = 6$ per group. $^{**}P \leq 0.01$ vs. the matched APE1 WT group; $^{\#}P \leq 0.05$; $^{\#\#\#}P \leq 0.001$ vs. the sham group.

TUNEL$^+$. Furthermore, microglia and astrocytes in the CC/EC were largely TUNEL$^-$ after 30 min of tFCI in both groups of animals (Fig. S4). Similarly, in the striatum (another white matter-enriched region) of postischemic APE1 cKO mice, the number of TUNEL$^+$/APC$^+$ cells was remarkably greater than in APE1 WT postischemic striatum (Fig. S5*A*). These data suggest that mature oligodendrocytes and neurons represent vulnerable cell populations in the white matter and gray matter of APE1-deficient mice, respectively.

DNA damage may activate the protein poly(ADP ribose) polymerase 1 (PARP1), which catalyzes the formation of poly(ADP ribose) polymers (PAR) using NAD$^+$ as substrate, thus eliciting intracellular NAD$^+$ and ATP depletion (21). PAR is a death signal in neurons after ischemia and reperfusion (23). Therefore, we assessed PAR immunoreactivity—evidence of PARP1 activity—in CC/EC protein extracts after tFCI. As expected, APE1 cKO mice had significantly higher levels of PAR in the CC/EC compared with APE1 WT mice (Fig. 5 *E* and *F*). Similar results were observed in the striatum (Fig. S5*C*). As shown by double-label immunofluorescence, PAR was largely localized to nuclei of APC$^+$ cells in the CC/EC (Fig. 5*G*) at 48 h after tFCI, whereas PAR immunofluorescence was elevated in both APC$^+$ and APC$^-$ cells in the postischemic striatum (Fig. S5*B*). Nevertheless, the number of PAR$^+$/APC$^+$ cells was markedly greater in both the CC/EC (Fig. 5*H*) and striatum (Fig. S5*B*) of APE1 cKO mice after tFCI when compared with APE1 WT mice. Taken together, these findings suggest that compromised DNA repair in APE1 cKO mice leads to the activation of the prodeath PARP1 protein in mature oligodendrocytes after tFCI, which could promote ischemic WMI.

APE1 Deficiency Exacerbates Myelin Loss and White Matter Dysfunction After Mild Ischemic Injury. Functional assessments of white matter are becoming increasingly prevalent in stroke studies, as histological assessments of gray matter do not always coincide with changes in behavioral functions. Using histological indicators

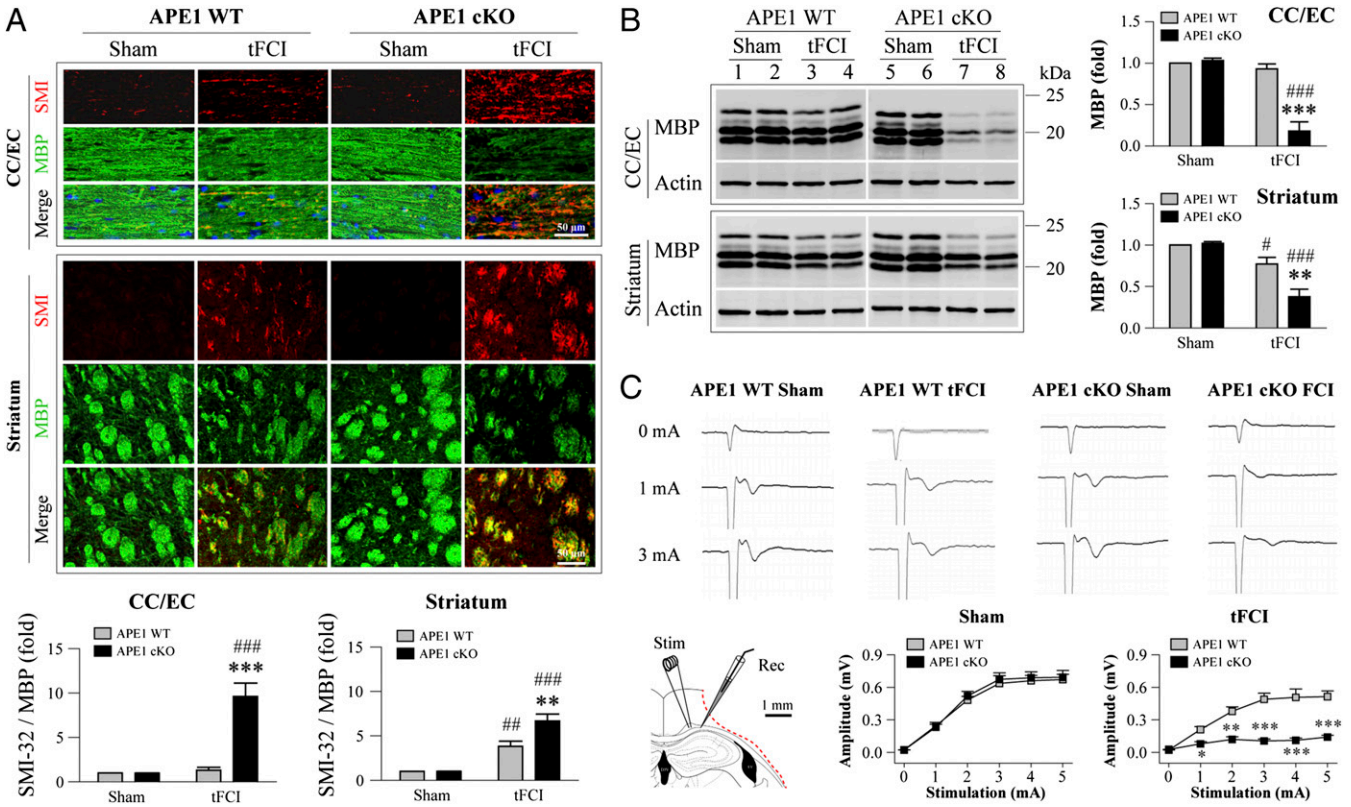

Fig. 6. APE1 deficiency elicits long-term loss of white matter integrity after tFCI. (*A*) Double-label immunofluorescent staining for MBP and dephosphorylated neurofilament protein (SMI-32) in the ipsilesional CC/EC and striatum at 28 d after 30 min of tFCI or sham operation. tFCI decreased MBP labeling and increased SMI-32 labeling in both CC/EC and striatum; APE1 cKO mice were much more affected than APE1 WT mice. The graphs at the bottom illustrate the ratio of SMI-32 to MBP, indicating the degree of demyelination in the CC/EC and striatum. Values are mean ± SEM, $n = 6$ per group. $^{**}P \leq 0.01$; $^{***}P \leq 0.001$ vs. the matched APE1 WT group; $^{\#\#}P \leq 0.01$; $^{\#\#\#}P \leq 0.001$ vs. sham group. (*B*) Western blot analysis showing multiple MBP bands in protein extracts from the CC/EC or striatum at 28 d after 30 min tFCI or sham operation. The graphs (*Right*) illustrate fold-changes in MBP protein levels in the CC/EC and striatum after tFCI relative to the sham group. Values were summed for all bands in each lane and are presented as mean ± SEM, $n = 4$–5 per group. $^{**}P \leq 0.01$; $^{***}P \leq 0.001$ vs. the matched APE1 WT group; $^{\#}P \leq 0.05$; $^{\#\#\#}P \leq 0.001$ vs. sham group. (*C*) Functional evaluation of white matter integrity by CAPs at 28 d after 30 min tFCI. The stimulating and recording electrodes were positioned in the CC of coronal brain slices to measure evoked CAPs (a dashed line indicates the approximate location of ischemic lesion). Representative traces of the evoked CAPs in the CC after subthreshold stimuli (labeled as 0), and 1- and 3-mA stimuli are shown. Signal conduction along nerve fibers, as measured by the amplitude of the N1 component of the CAPs in response to increasing stimulus strength (up to 5 mA) were analyzed in sham controls and after tFCI. Data are mean ± SEM, $n = 6$–8 per group. $^{*}P \leq 0.05$; $^{**}P \leq 0.01$; $^{***}P \leq 0.001$ vs. the matched APE1 WT group.

of white matter integrity, we examined the impact of APE1 knockout on WMI 28 d after 30 min of tFCI. For these studies we relied on immunohistochemical staining with the SMI-32 antibody, which recognizes the nonphosphorylated epitope of neurofilament H, a robust marker of demyelination (24). Under sham control conditions, faint staining with SMI-32 was visible in the CC/EC region and striatum (Fig. 6*A*). In APE1 WT mice, striatal SMI-32 immunoreactivity was enhanced after tFCI, resulting in an increased ratio of SMI-32 to myelin basic protein (MBP) (Fig. 6*A*). In contrast, no changes were detected in the CC/EC of these animals, suggesting that this region lay outside the zone of permanent WMI following mild ischemic injury. In APE1 cKO mice, a dramatic increase in SMI-32 immunoreactivity was evident in both the CC/EC and fascicles of the striatal internal capsule after tFCI, suggesting an expansion of the zone of permanent WMI (Fig. 6*A*). A simultaneous reduction in the intensity of MBP was observed in the postischemic brain of APE1 cKO mice, most notably along the fiber tracts of the CC/EC (Fig. 6*A*), indicating a loss of white matter myelination. Accordingly, the ratio of SMI-32 to MBP was markedly increased in the CC/EC and striatum of APE1 cKO mice compared with the APE1 WT mice after tFCI (Fig. 6*A*). Western blots on tissue lysates from the CC/EC and striatum showed a dramatic reduction in MBP expression in both regions after tFCI in APE1 cKO mice compared with APE1 WT mice (Fig. 6*B* and Fig. S6).

The immunohistochemical detection of white matter markers described above demonstrates that the loss of APE1 enhances demyelination after ischemia. Therefore, we sought to determine if increased demyelination of the white matter tracts led to a loss in the functional integrity of white matter. Using electrophysiological assessments of compound action potentials in the CC/EC from coronal brain slices harvested 28 d after 30 min of tFCI, we found a significant reduction in the peak amplitude in APE1 cKO mice (Fig. 6*C*), reflecting impairments in conduction along myelinated axons. This effect was not evident in sham controls of the APE1 cKO mice or the APE1 WT mice after tFCI. Taken together, the data suggest that APE1 protects against the development of postischemic infarction and is critical for the structural preservation of gray and white matter and the recovery of behavioral function after mild ischemic injury.

Discussion

To our knowledge, the present study provides the first direct evidence that endogenous APE1 naturally blunts the progression of gray and white matter injury in experimental stroke and facilitates poststroke functional recovery. Four major findings from this study contribute to our understanding of the role of DNA repair in the intrinsic recovery process after cerebral ischemia and reperfusion. First, the loss of APE1 largely prevents the intrinsic repair of AP

sites in gray matter and promotes the accumulation of ODD in the form of AP sites and strand breaks in the postischemic brain. Second, loss of APE1 dramatically exacerbates ischemic cell death of neurons and oligodendrocytes, probably through activation of distinct cell death programs, such as PARP1- and PUMA-dependent signaling pathways. Third, the loss of APE1 augments postischemic demyelination and white matter dysfunction. Fourth, the loss of APE1 inhibits the endogenous recovery of sensorimotor function and spatial learning and memory under mild injury conditions.

Historically, the role of endogenous APE1 has been difficult to assess, particularly in targeted structures, such as the brain or in specific cellular subtypes. The conventional global knockout of APE1 causes early embryonic lethality (15, 17), which both underscores its essential role in cell survival and creates an impediment to studying its function in adult animals. Several techniques have been used to generate APE deletion models, including RNA interference and the generation of APE1 knockout cells that survive because of the coexpression of human APE1 under a conditional promoter (14, 25). However, these models only have limited applicability in animal studies. By creating a conditional APE1 knockout mouse that allows for disruption of the APE1 gene in adulthood, we have demonstrated here that APE1 unequivocally contributes to endogenous neuroprotection against ischemic injury in vivo, validating it as a potential target in neurotherapeutic strategies. A robust exacerbation of ischemic injury was evident in APE1 cKO mice, not only promoting cell death in gray and white matter, but also extending to behavioral outcomes. Although the data contribute to our understanding of the role of DNA repair in cellular recovery from cerebral ischemia, the use of this APE1 cKO mouse line could easily be extended to other models, including genesis of chemotherapy-resistant tumors in different cellular subtypes, traumatic CNS injury, aging and neurodegenerative diseases, mitochondrial DNA repair, and so forth.

Our data consistently demonstrate that APE1 knockout mice exhibit worse outcomes following transient cerebral ischemia. This observation could be interpreted as arising from two distinct mechanisms that are not mutually exclusive. First, given that the mortality rate after moderate (60 min) ischemia was higher in APE1 knockout mice, the loss of APE1 before the insult could potentiate cellular injury by creating a baseline level of unrepaired ODD that rises above a lethality threshold upon ischemic injury. This stressful baseline environment might be considered an "aging-like" phenotype, wherein accumulation of ODD sensitizes the system to subsequent oxidative insults, such as ischemia. Alternatively, ischemic injury and ODD might induce APE1 activity immediately following reperfusion, especially in those cells that are not severely injured or are located in the penumbra. The loss of APE1 would then represent a failure in postischemic recovery that may be independent of a predisposition, as implied in the first scenario. In either scenario, the repair of ODD would be essential to eventual structural and functional recovery. Both alternatives are consistent with a prolonged accumulation of AP sites and DNA strand breaks in ischemic APE1 knockout animals. Further studies to distinguish between the two alternatives are warranted.

The molecular mechanisms underlying WMI after stroke and the roles of APE1/DNA repair in this process have only recently begun to be explored. White matter is remarkably sensitive to ischemic injury (26), and white matter repair may be critical to improving functional recovery following cerebral ischemia. Our data demonstrate that APE1 promotes the survival of oligodendrocytes and both the structural and functional integrity of white matter after a transient ischemic episode. These data support the concept that white matter mounts a programmed response to ischemic injury and that APE1 is a major component of a white matter self-defense and self-repair program. Future studies targeting APE1 knockout specifically to white matter cell populations, such as the myelin-producing oligodendrocytes, may help verify the role of white matter injury and repair in postischemic outcomes and potentially lead to new therapeutic strategies that encompass both gray and white matter.

Our data suggest that the loss of APE1 leads to the activation of two distinct prodeath signaling pathways, PUMA and PARP1, which may underlie pathological events following ODD accumulation. The potentiation of ischemic WMI by compromised DNA repair (or the lack of adequate recovery) appears to be primarily associated with PARP1 activation. Whether the activation of PARP1 in white matter reflects a secondary or bystander cell death process in response to neuronal injury is still unknown, but can be addressed by further studies using cell-specific approaches. The neuronal activation of PUMA in the ischemic cortex represents a proapoptotic process that demands energy (27), thus indicating that the molecular mechanisms underpinning the ischemic response by neurons may be intrinsically different from in the white matter because of distinct energy reserves or capacities. In contrast to PUMA, PARP1 activation is generally associated with necrosis and catastrophic depletion of energy stores.

A parsimonious explanation of the observed regional differences between the striatum and cortex is differences in the degree of blood flow interruption during the stroke event itself. In this context, induction of APE1 is well established in sublethal injury models (5, 28). Therefore, regions that lie proximal versus distal to the ischemic core may rely differentially on APE1. Other topographical differences between the striatum and cortex, such as unique efferent and afferent projections, heterogeneity in glial subpopulations, and differential expression of neurotransmitters and prosurvival proteins, might contribute somewhat to the regionally selective responses to ischemic injury in the APE1 knockout mouse. Further investigations using cell and region-specific targeting of APE1 knockout could help address these questions and better define mechanisms associated with specific cell subtypes (neurons, astrocytes, oligodendrocytes, endothelial cells, and so forth) and with topographically selective vulnerabilities. The new conditional APE1 knockout model described here offers a novel platform on which to rigorously examine these important variables in greater mechanistic depth.

Although best characterized for its DNA repair function, APE1 also contains a highly sensitive redox region that is dependent on a cysteine residue within its N-terminal region (29). Several studies implicate this region in influencing the activity of a number of transcription factors, such as AP-1, Myb, NF-κB, HIF-1α, ATF/CREB, p53, and so forth (reviewed in ref. 28), and indicate that the redox function of APE1 acts independently of DNA repair activity. Our current model explored a relatively acute timeframe following cerebral ischemia and correlated the loss of APE1 with accumulation of ODD. However, it is possible that deleterious outcomes following a transient ischemic insult in the APE1 knockout mouse may be influenced by the lack of the redox action of APE1 in addition to its role in DNA repair. Comparison of the effects of gene knock-in of APE1 containing point mutations of the redox-active site versus of the DNA repair-competent site would be a logical progression for future studies. It should be noted here that overexpression of exogenous APE1 with a mutated DNA repair site but an intact redox site does abolish its protective effects against ischemia (10), indicating that the repair function is indeed critical for protection against ischemic injury.

We have provided evidence that cKO of APE1 in the adult mice exacerbates ischemic injury in both gray and white matter, perhaps via topographically distinct activation of prodeath signaling pathways. To our knowledge these data provide the first animal model of targeted APE1 knockout and support the engagement of multiple distinct cell death mechanisms following cerebral ischemia. The defensive role of endogenous APE1 in stroke is consistent with human studies showing that single nucleotide polymorphisms in the APE1 gene are associated with greater risk for cerebral ischemic infarction (30). Further studies assessing the role of DNA repair in specific cell types in the brain and under

different injury conditions may accelerate the development of successful therapeutic interventions for stroke victims.

Methods

Generation of Conditional APE1 Knockout Mice. APE1$^{flox/flox}$ mice were generated on a C57BL/6J background as described in *SI Methods*. To obtain conditional APE1 knockout mice, homozygous APE1$^{flox/flox}$ mice were crossed with hemizygous CAGGCre-ER mice (The Jackson Laboratory), in which the Cre-mediated recombination is controlled by tamoxifen and is ubiquitous in all tissues (18). CAGGCre-ER; APE1$^{flox/flox}$ mice were obtained after at least two generations of crossing (Fig. S2*A*) and transformed into conditional APE1 knockout (APE1 cKO) animals following tamoxifen injections (75 mg/kg, i.p., once a day for 5 d). Mice with the genotype of CAGGCre-ER; APE$^{wt/wt}$ were used as controls (APE1 WT) (Fig. S2*B*) and received the same tamoxifen treatment regimen in all studies. Induced knockout of APE1 was confirmed by Western blotting (Fig. S2*D*).

Transient Focal Cerebral Ischemia Model. Twenty-four hours after the last tamoxifen injection, tFCI was induced in adult male mice (8–10 wk old, 25–30 g) by intraluminal occlusion of the left middle cerebral artery, as described previously (31). Surgeries and all outcome assessments were performed by investigators blinded to mouse genotype and experimental group assignments. All animal procedures were approved by the University of Pittsburgh Institutional Animal Care and Use Committee, and performed to NIH guidelines.

Neurofunctional Assessments. Neurobehavioral tests were carried out 3 d before and 1–28 d after tFCI. Sensorimotor deficits were evaluated by the rotarod and corner tests. Cognitive deficits were evaluated by the Morris water maze test.

Assessment of Gray and WMI. Details of histological assessments for brain injury are further described in *SI Methods*. Neuronal (i.e., gray matter) injury was assessed by MAP2 immunostaining (28 d following tFCI) and by double-label immunofluorescent staining for NeuN and the DNA damage marker p-H2AX (2 h and 24 h following tFCI) or TUNEL (24 h following tFCI). WMI induced by tFCI was examined at the histological and functional levels. Free-floating coronal brain sections (30 μm) were processed for immunostaining with MBP and SMI-32 antibodies. White matter damage was quantitated as the ratio of SMI-32 to MBP immunostaining relative to sham animals. The functional integrity of white matter was assessed by measuring compound action potentials (CAPs) in the CC and EC of coronal brain slices (350-μm thick), as described previously (32).

Assessment of ODD. DNA SSB were detected on fixed coronal brain sections using DNA PANT, as described previously (3). PANT^{+} cells were stereologically quantified by a blinded investigator. Contents of AP sites were measured with the biotin-labeled aldehyde reactive probe in a colorimetric assay (10).

Statistical Analyses. Data are presented as mean ± SEM. Differences between means from two groups were analyzed by the Student's *t* test (two-tailed). Differences in means from multiple groups were analyzed using one- or two-way ANOVA followed by the Bonferroni/Dunn post hoc correction. Comparisons of animal survival rates were performed by Kaplan–Meier survival analysis. A *P* value less than 0.05 was deemed statistically significant.

ACKNOWLEDGMENTS. We thank Ed Mallick for technical assistance in generating the apurinic/apyrimidinic endonuclease-1 conditional knockout mouse line. This research was supported by National Institutes of Health Grants NS036736, NS045048, and NS089534 (to J.C.), NS45287 (to M.V.L.B.), and AA10422 (to G.E.H); a US Department of Veterans Affairs Senior Research Career Scientist Award (to J.C.); Chinese Natural Science Foundation Grants 81020108021, 81171149, and 81371306 (to Y.G.), and 81228008 (to J.C.); and the High-end Distinguished Professorship GDW20133100069 from the State Administration of Foreign Experts Affairs of China (to M.V.L.B.).

1. Nagayama T, et al. (2000) Activation of poly(ADP-ribose) polymerase in the rat hippocampus may contribute to cellular recovery following sublethal transient global ischemia. *J Neurochem* 74(4):1636–1645.
2. Schwamm LH, et al. (1998) Time course of lesion development in patients with acute stroke: Serial diffusion- and hemodynamic-weighted magnetic resonance imaging. *Stroke* 29(11):2268–2276.
3. Chen J, et al. (1997) Early detection of DNA strand breaks in the brain after transient focal ischemia: Implications for the role of DNA damage in apoptosis and neuronal cell death. *J Neurochem* 69(1):232–245.
4. Lan J, et al. (2003) Inducible repair of oxidative DNA lesions in the rat brain after transient focal ischemia and reperfusion. *J Cereb Blood Flow Metab* 23(11):1324–1339.
5. Li W, et al. (2006) Ischemic preconditioning in the rat brain enhances the repair of endogenous oxidative DNA damage by activating the base-excision repair pathway. *J Cereb Blood Flow Metab* 26(2):181–198.
6. Ljungquist S, Lindahl T (1974) A mammalian endonuclease specific for apurinic sites in double-stranded deoxyribonucleic acid. I. Purification and general properties. *J Biol Chem* 249(5):1530–1535.
7. Ljungquist S, Andersson A, Lindahl T (1974) A mammalian endonuclease specific for apurinic sites in double-stranded deoxyribonucleic acid. II. Further studies on the substrate specificity. *J Biol Chem* 249(5):1536–1540.
8. Srivastava DK, et al. (1998) Mammalian abasic site base excision repair. Identification of the reaction sequence and rate-determining steps. *J Biol Chem* 273(33):21203–21209.
9. Kawase M, Fujimura M, Morita-Fujimura Y, Chan PH (1999) Reduction of apurinic/apyrimidinic endonuclease expression after transient global cerebral ischemia in rats: Implication of the failure of DNA repair in neuronal apoptosis. *Stroke* 30(2):441–448, discussion 449.
10. Leak RK, et al. (2015) Apurinic/apyrimidinic endonuclease 1 upregulation reduces oxidative DNA damage and protects hippocampal neurons from ischemic injury. *Antioxid Redox Signal* 22(2):135–148.
11. Kim HW, Cho KJ, Park SC, Kim HJ, Kim GW (2009) The adenoviral vector-mediated increase in apurinic/apyrimidinic endonuclease inhibits the induction of neuronal cell death after transient ischemic stroke in mice. *Brain Res* 1274:1–10.
12. Stetler RA, et al. (2010) Apurinic/apyrimidinic endonuclease APE1 is required for PACAP-induced neuroprotection against global cerebral ischemia. *Proc Natl Acad Sci USA* 107(7):3204–3209.
13. Morita-Fujimura Y, Fujimura M, Kawase M, Chan PH (1999) Early decrease in apurinic/apyrimidinic endonuclease is followed by DNA fragmentation after cold injury-induced brain trauma in mice. *Neuroscience* 93(4):1465–1473.
14. Vasko MR, Guo C, Kelley MR (2005) The multifunctional DNA repair/redox enzyme Ape1/Ref-1 promotes survival of neurons after oxidative stress. *DNA Repair (Amst)* 4(3):367–379.
15. Ludwig DL, et al. (1998) A murine AP-endonuclease gene-targeted deficiency with post-implantation embryonic progression and ionizing radiation sensitivity. *Mutat Res* 409(1):17–29.
16. Singh S, Englander EW (2012) Nuclear depletion of apurinic/apyrimidinic endonuclease 1 (Ape1/Ref-1) is an indicator of energy disruption in neurons. *Free Radic Biol Med* 53(9):1782–1790.
17. Xanthoudakis S, Smeyne RJ, Wallace JD, Curran T (1996) The redox/DNA repair protein, Ref-1, is essential for early embryonic development in mice. *Proc Natl Acad Sci USA* 93(17):8919–8923.
18. Hayashi S, McMahon AP (2002) Efficient recombination in diverse tissues by a tamoxifen-inducible form of Cre: A tool for temporally regulated gene activation/inactivation in the mouse. *Dev Biol* 244(2):305–318.
19. Guillet M, Boiteux S (2002) Endogenous DNA abasic sites cause cell death in the absence of Apn1, Apn2 and Rad1/Rad10 in *Saccharomyces cerevisiae*. *EMBO J* 21(11):2833–2841.
20. Paull TT, et al. (2000) A critical role for histone H2AX in recruitment of repair factors to nuclear foci after DNA damage. *Curr Biol* 10(15):886–895.
21. Li P, et al. (2011) Mechanistic insight into DNA damage and repair in ischemic stroke: Exploiting the base excision repair pathway as a model of neuroprotection. *Antioxid Redox Signal* 14(10):1905–1918.
22. Kissela B, et al. (2009) Clinical prediction of functional outcome after ischemic stroke: The surprising importance of periventricular white matter disease and race. *Stroke* 40(2):530–536.
23. Andrabi SA, et al. (2006) Poly(ADP-ribose) (PAR) polymer is a death signal. *Proc Natl Acad Sci USA* 103(48):18308–18313.
24. Trapp BD, et al. (1998) Axonal transection in the lesions of multiple sclerosis. *N Engl J Med* 338(5):278–285.
25. Izumi T, et al. (2005) Two essential but distinct functions of the mammalian abasic endonuclease. *Proc Natl Acad Sci USA* 102(16):5739–5743.
26. Pantoni L, Garcia JH, Gutierrez JA (1996) Cerebral white matter is highly vulnerable to ischemia. *Stroke* 27(9):1641–1646, discussion 1647.
27. Nakano K, Vousden KH (2001) PUMA, a novel proapoptotic gene, is induced by p53. *Mol Cell* 7(3):683–694.
28. Tell G, Quadrifoglio F, Tiribelli C, Kelley MR (2009) The many functions of APE1/Ref-1: Not only a DNA repair enzyme. *Antioxid Redox Signal* 11(3):601–620.
29. Xanthoudakis S, Curran T (1992) Identification and characterization of Ref-1, a nuclear protein that facilitates AP-1 DNA-binding activity. *EMBO J* 11(2):653–665.
30. Naganuma T, et al. (2009) Haplotype-based case-control study between human apurinic/apyrimidinic endonuclease 1/redox effector factor-1 gene and cerebral infarction. *Clin Biochem* 42(15):1493–1499.
31. Stetler RA, et al. (2008) Hsp27 protects against ischemic brain injury via attenuation of a novel stress-response cascade upstream of mitochondrial cell death signaling. *J Neurosci* 28(49):13038–13055.
32. Wang G, et al. (2015) HDAC inhibition prevents white matter injury by modulating microglia/macrophage polarization through the GSK3β/PTEN/Akt axis. *Proc Natl Acad Sci USA* 112(9):2853–2858.
33. Ferguson C, et al. (2007) New insight into the role of the beta3 subunit of the GABAA-R in development, behavior, body weight regulation, and anesthesia revealed by conditional gene knockout. *BMC Neurosci* 8:85.
34. Akiyama K, et al. (1995) Cloning, sequence analysis, and chromosomal assignment of the mouse Apex gene. *Genomics* 26(1):63–69.

35. Nagy A, Rossant J, Nagy R, Abramow-Newerly W, Roder JC (1993) Derivation of completely cell culture-derived mice from early-passage embryonic stem cells. *Proc Natl Acad Sci USA* 90(18):8424–8428.
36. Committee on Care and Use of Laboratory Animals (1996) *Guide for the Care and Use of Laboratory Animals* (National Institutes of Health, Bethesda, MD), DHHS Publ No (NIH) 85-23.
37. Fisher M, et al.; STAIR Group (2009) Update of the stroke therapy academic industry roundtable preclinical recommendations. *Stroke* 40(6):2244–2250.
38. Li P, et al. (2013) Adoptive regulatory T-cell therapy preserves systemic immune homeostasis after cerebral ischemia. *Stroke* 44(12):3509–3515.
39. Gan Y, et al. (2012) Transgenic overexpression of peroxiredoxin-2 attenuates ischemic neuronal injury via suppression of a redox-sensitive pro-death signaling pathway. *Antioxid Redox Signal* 17(5):719–732.
40. Leak RK, et al. (2013) HSP27 protects the blood-brain barrier against ischemia-induced loss of integrity. *CNS Neurol Disord Drug Targets* 12(3):325–337.
41. Fancy SP, et al. (2014) Parallel states of pathological Wnt signaling in neonatal brain injury and colon cancer. *Nat Neurosci* 17(4):506–512.
42. Cao G, et al. (2007) Critical role of calpain I in mitochondrial release of apoptosis-inducing factor in ischemic neuronal injury. *J Neurosci* 27(35):9278–9293.
43. Zhang F, et al. (2012) Pharmacological induction of heme oxygenase-1 by a triterpenoid protects neurons against ischemic injury. *Stroke* 43(5):1390–1397.
44. Zhang L, et al. (2002) A test for detecting long-term sensorimotor dysfunction in the mouse after focal cerebral ischemia. *J Neurosci Methods* 117(2):207–214.
45. Wang G, et al. (2013) Scriptaid, a novel histone deacetylase inhibitor, protects against traumatic brain injury via modulation of PTEN and AKT pathway:scriptaid protects against TBI via AKT. *Neurotherapeutics* 10(1):124–142.
46. Cao G, et al. (2001) Intracellular Bax translocation after transient cerebral ischemia: Implications for a role of the mitochondrial apoptotic signaling pathway in ischemic neuronal death. *J Cereb Blood Flow Metab* 21(4):321–333.
47. Karthigasan J, Garvey JS, Ramamurthy GV, Kirschner DA (1996) Immunolocalization of 17 and 21.5 kDa MBP isoforms in compact myelin and radial component. *J Neurocytol* 25(1):1–7.